Records of the $\delta^{13}C$ of atmospheric CH_4 over the last 2 centuries as recorded in Antarctic snow and ice

Todd Sowers

Department of Geosciences and the Earth and Environmental Systems Institute, Pennsylvania State University, University Park, Pennsylvania, USA

Sophie Bernard, Olivier Aballain, Jérôme Chappellaz, and Jean-Marc Barnola

Laboratoire de Glaciologie et Géophysique de l'Environnement, St. Martin d'Hères, France

Thomas Marik

Institute of Environmental Physics, University of Heidelberg, Heidelberg, Germany

Received 9 November 2004; revised 26 January 2005; accepted 10 February 2005; published 2 April 2005.

[1] Methane is one of the important greenhouse gases accumulating in the atmosphere today. The increased loading over the past 2 centuries is thought to be the result of increased anthropogenic emissions. Here we present records of the $\delta^{13}C$ of CH_4 in firn air from the South Pole and in trapped bubbles in a short ice core from Siple Dome, Antarctica, that help constrain historical emissions of various sources throughout the last 2 centuries. Using two firn air samplings in 1995 and 2001 we calculate that $\delta^{13}CH_4$ has increased by an average of 0.06 ± 0.02‰/yr over the 6 years between samplings. Our ice core results suggest the $\delta^{13}C$ of atmospheric CH_4 has increased by 1.8 ± 0.2‰ between 1820 A.D. and 2001 AD. The $\delta^{13}CH_4$ changes in both data sets are the result of an increase in the relative proportion of CH_4 sources with elevated $^{13}C/^{12}C$ isotope ratios. One explanation for observed trends involves a 16 Tg/yr increase in CH_4 emissions associated with biomass burning over the past 2 centuries.

Citation: Sowers, T., S. Bernard, O. Aballain, J. Chappellaz, J.-M. Barnola, and T. Marik (2005), Records of the $\delta^{13}C$ of atmospheric CH_4 over the last 2 centuries as recorded in Antarctic snow and ice, *Global Biogeochem. Cycles*, *19*, GB2002, doi:10.1029/2004GB002408.

1. Introduction

[2] Methane (CH_4) is a greenhouse gas that is currently accumulating in the atmosphere at a rate (now declining) of about 0.4% per year. Over the past 2 centuries, the atmospheric CH_4 concentration has doubled in response to increasing anthropogenic related emissions. The primary anthropogenic CH_4 sources are ruminants, rice paddies, landfills, natural gas release, and biomass burning. The largest natural source is wetlands followed by natural fires, termites, and oceanic emissions including clathrate destabilization (for a thorough review, see *Reeburgh* [2004]). The total CH_4 source strength at any point in time can be estimated knowing the rate at which CH_4 accumulates in the atmosphere and the loss of CH_4 via OH oxidation in the troposphere. This exercise does not, however, provide any information about the relative contributions of the various sources. In order to refine estimates of the magnitude of each individual source, measurements of the $\delta^{13}C$ of atmospheric CH_4 ($\delta^{13}CH_4$) have been made. Knowing the characteristic isotope composition of the various sources, one can improve our understanding of the historical emissions with a $\delta^{13}CH_4$ record in hand. Information of this type is important as we estimate future climate change that may result from anthropogenically mediated changes in the Earth's radiation budget [*Hansen et al.*, 2000].

1.1. Previous Studies of Recent Atmospheric Methane Trends

[3] Ice cores provide the primary means of reconstructing the composition of past atmospheres. High-resolution atmospheric records have been reconstructed for the last 1000 years from the Law Dome ice cores [*Etheridge et al.*, 1998]. Methane concentration records from Law Dome have documented atmospheric loadings that have increased in an exponential fashion starting from ~670 ppb in 1000 A.D. to ~1600 ppb in 1970 A.D. The major cause of this increase is thought to be the result of anthropogenic emissions (rice, cattle, biomass burning, and fossil fuels) with a smaller contribution from a net reduction in the primary atmospheric sink (tropospheric OH).

[4] To date, only one set of ice core analyses have been made to estimate the $\delta^{13}C$ of paleoatmospheric CH_4. *Craig et al.* [1988] made $\delta^{13}CH_4$ measurements on large ice samples from the Crete ice core (central Greenland) and concluded that atmospheric $\delta^{13}CH_4$ increased by ~2‰ over the past 2 centuries. Unfortunately, *Craig et al.* [1988]

0886-6236/05/2004GB002408$12.00

failed to account for a number of important factors (gas age−ice age difference, gravitational and thermal fractionation, and the diffusional impact of increasing $[CH_4]$ on the $\delta^{13}CH_4$ of firn air CH_4) making their estimates of the net change in atmospheric $\delta^{13}CH_4$ uncertain though the sense of the change is probably correct.

[5] Analyses of air from the interstitial spaces around snow near the surface of polar ice sheets (firn air) provides the means of splicing ice core records with direct measurements of the troposphere which began in the 1950s. Firn air $\delta^{13}CH_4$ measurements indicate a positive recent trend of 0.03−0.10‰ per year for the later part of the twentieth century [*Bräunlich et al.*, 2001; *Francey et al.*, 1999]. By way of comparison, the current peak-to-peak amplitude of the seasonal $\delta^{13}CH_4$ variations range from 0.1 to 0.4‰ in both hemispheres while the pole-to-pole difference is ∼0.5‰ with a tendency toward larger gradients during the boreal winter [*Lowe et al.*, 1999; *Platt et al.*, 2004; *Quay et al.*, 1999; *Rice et al.*, 2001]. Since loss of CH_4 is controlled primarily by reaction with OH in the troposphere, the potential influence of isotope effects associated with loss processes in the stratosphere has been omitted in a number of budget studies [e.g., *Craig et al.*, 1988; *Francey et al.*, 1999]. *Gupta et al.* [1996] pointed out, however, that the increase in the stratospheric Cl (with concomitant CH_4 removal) should have raised tropospheric $\delta^{13}CH_4$ by as much as 0.7‰ over the past century. Estimates suggest that stratospheric Cl loading may have increased by ∼200% owing to the introduction of chlorine containing freons [*Flocke et al.*, 1999]. The magnitude of the Cl impact on tropospheric $\delta^{13}CH_4$ has been recently reassessed indicating the net impact is probably between 0.2 and 0.5‰ [*McCarthy et al.*, 2003; *Wang et al.*, 2002].

[6] Recently, measurements of firn air from Dome C and Dronning Maud Land have yielded new $\delta^{13}CH_4$ data that extend the atmospheric record back to ∼1950 A.D. Results indicate the $\delta^{13}CH_4$ in the far Southern Hemisphere has increased by ∼1.7‰ since 1950 A.D. The trend toward higher $\delta^{13}CH_4$ was thought to be the result of increased CH_4 emissions from biomass burning and fossil fuel consumption [*Bräunlich et al.*, 2001].

[7] The present contribution extends the atmospheric record to the early 1900s with analyses of firn air from the South Pole that were drawn in January 1995 and 2001 [*Battle et al.*, 1996]. Additionally, samples from a shallow ice core from the Siple Dome area are used to establish the $\delta^{13}CH_4$ value during the nineteenth century. Moreover, the two separate firn air samplings provide an opportunity to establish the evolution of the firn air profiles over a 6-year period from the same locale. In the sections that follow, we initially discuss how firn air from South Pole has been sampled and used to reconstruct atmospheric records over the past century. We then discuss the methods we used to measure $\delta^{13}CH_4$ and present results from two separate South Pole sampling expeditions measured in two labs. In order to establish a preanthropogenic $\delta^{13}CH_4$ value, a new technique was developed to extract and analyze the $\delta^{13}CH_4$ of air trapped in ice from a shallow core at Siple Dome. Finally, we discuss the significance of the results in terms of estimating historical CH_4 emissions from anthropogenically mediated biomass burning.

1.2. Retrieving Interstitial Air From Polar Snow

[8] The composition of air within the interstitial spaces in polar snowfields is dictated by the historical atmospheric record and the rate at which air mixes in a vertical sense [*Schwander et al.*, 1993]. At the South Pole, the firn/ice transition is located ∼123 m below the surface (mbs) [*Battle et al.*, 1996]. Below 123 mbs, air is occluded in bubbles and can no longer communicate with the overlying atmosphere. Firn air at the South Pole is reasonably well mixed in the upper 2−5 m by wind and atmospheric pressure changes. Below 5 m, the air mixes solely by diffusion down to ∼116 m, corresponding to the top of the "lock-in" zone [*Battle et al.*, 1996]. At this depth, the open porosity decreases to a level where the tortuous nature of the firn no longer allows the air within the lock-in zone to mix with the overlying firn air. The air becomes effectively sealed in the firn although very few bubbles are apparent. Below 116 m, the age of the air increases with depth at a rate that is dictated by the snow accumulation rate (∼8 cm of ice equivalent/year).

[9] Over time, atmospheric compositional changes are propagated down into the firn by diffusion. At the South Pole, the average age of CH_4 molecules just above the bubble close-off region date to ∼1900 A.D. Moving up the firn column, the age of the air decreases rapidly between 123 and 116 m and then more slowly from 116 m to the surface. The composition of the air at any depth in the firn is therefore dependent on the atmospheric history and the diffusion processes controlling the movement of each constituent down into the firn [*Battle et al.*, 1996].

[10] Two separate expeditions were mounted to retrieve firn air from the geographic South Pole. The first expedition occurred in January of 1995 where two holes (30 m apart) were drilled incrementally and sampled at 30 different depths using standard techniques to fill replicate flasks [*Battle et al.*, 1996; *Schwander et al.*, 1993]. In January 2001, a similar expedition was mounted using effectively the same equipment. In 2001, two additional holes were drilled incrementally and sampled at a total of 31 depths. A subset of flasks from both experiments was measured at NOAA/CMDL for trace gas species. Another suite of flasks was measured at Princeton for the elemental and isotopic composition of O_2, N_2, and Ar. The results from these analyses provide the basis for the firn air modeling that we discuss in a later section.

2. Analytical Methodology for Measuring $\delta^{13}C$ of CH_4

2.1. LGGE Analyses

[11] The $\delta^{13}C$ measurements at LGGE were made with a Finnigan MAT 252 mass spectrometer coupled to a Finnigan GC/combustion interface in continuous flow mode (CF-IRMS). CH_4 was initially isolated from other air constituents using a preconcentration device. Air samples are initially expanded into a pre-evacuated 150-mL sample loop that is subsequently flushed with pure He carrier gas for 20 min at 70 mL/min. The He carrier stream was

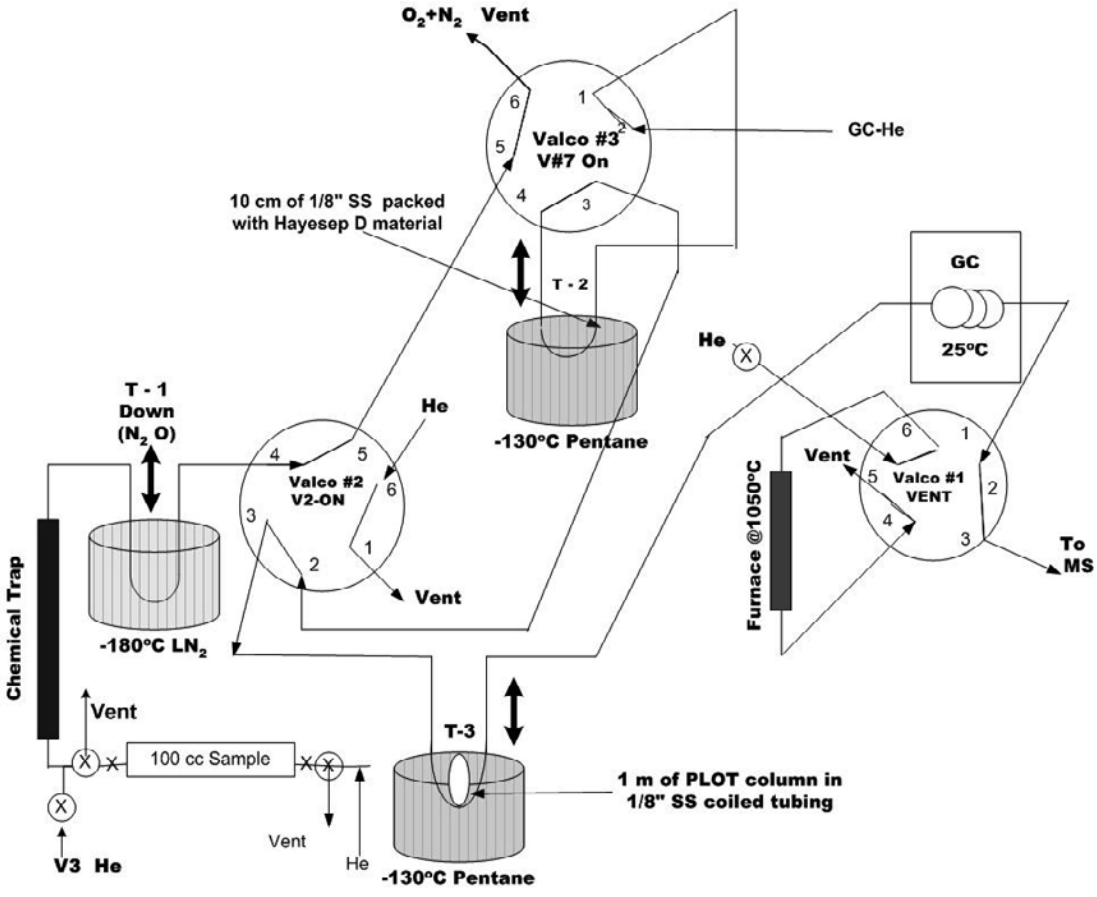

Figure 1. Schematic of the PSU preconcentration system.

passed through a HaySep D column (80/100 mesh, 20 cm length, 0.32cm OD) held at −130°C to trap CH_4 and CO_2 with the remainder of the air/He directed to vent. A six port Valco valve is then switched before the HaySep D column is instantaneously warmed to 50°C to release the trapped CH_4 sample and other condensable gases from the HaySep D column. The CH_4 and CO_2 were then cryofocused onto a 3-m capillary column (fused silica Poraplot Q, 0.32 mm ID) at −130°C. Finally, the focusing column was warmed to 50°C to release the CH_4 and CO_2 into a 30-m Poraplot Q column where the CH_4 was separated from CO_2 and N_2O. The effluent from the Poraplot column was then fed into an oxidation furnace (Ni, Pt, and Cu at 980°C) where CH_4 was converted to CO_2. The sample stream then passes through a reduction oven to remove N_2O and O_2 from the effluent stream. After a drying stage (Nafion membrane), the sample was transferred to the mass spectrometer using an open split design, where about one third of the effluent from the chromatographic column was admitted via a capillary into the ion source. The mass to charge ratio (m/e) for the 44-, 45-, and 46-isotopologue peaks were integrated before the $^{13}C/^{12}C$ ratio was then calculated using the ^{17}O correction following *Santrock et al.* [1985]. The $\delta^{13}CH_4$ values were reported on the VPDB scale using a pure CO_2 working standard with a $\delta^{13}CH_4$ value of −45.98 ± 0.02‰. System checks are performed daily using a compressed air standard (CSIRO 1636) that was filled at Cape Grim on March 1995 in collaboration with the Commonwealth Scientific and Industrial Research Organisation (CSIRO), who subsequently determined the $\delta^{13}CH_4$ value as −47.12 ± 0.03‰. Throughout the 3 years over which measurements have been made at LGGE for this study, the average $\delta^{13}CH_4$ on this tank was −47.07 ± 0.18‰ (N = 201).

2.2. PSU Analyses

[12] At PSU, we have developed a CF-IRMS technique to measure the $\delta^{13}CH_4$ in air samples that is similar to previously developed techniques [*Miller et al.*, 2002; *Rice et al.*, 2001b]. The analytical system consists of a substantially modified PreCon device (Finnigan MAT) that interfaces with a MAT 252 mass spectrometer (Figure 1).

[13] The system was designed to measure $\delta^{13}C$ of CH_4 as well as the $\delta^{15}N$ and $\delta^{18}O$ of N_2O from a single air sample. The details of the N_2O analyses have been previously discussed [*Sowers et al.*, 2002]. Initially, samples are loaded onto the PreCon between two 1/4″ ultratorr adapters. The connections are flushed with He for 3 min (15 cc/min) before the glass valves on the 100-cc sample flask are opened allowing the air to be flushed (30 cc/min) into a chemical trap containing ascarite and $MgClO_4$ for CO_2 and H_2O removal. The air sample is then passed through a 1/32″ stainless steel (SS) loop in liquid nitrogen (LN_2) where the N_2O is trapped. The air +CH_4 stream is then routed through

Table 1. Accuracy and Precision of PSU Analytical Procedures[a]

Measured Quantity	N	$\delta^{13}C$, ‰ PDB	Measured − Accepted, ‰
Assigned $\delta^{13}CO_2$ for liquid standard (NIST)[b]	16	−33.26 ± 0.07	N/A
CH_4 Std#1 ([CH_4] = 1441 ppb, $\delta^{13}CH_4$ = −19.6‰)[c]	51	−19.6 ± 0.3	0.0 ± 0.3
CH_4 Std#2 ([CH_4] = 1776 ppb, $\delta^{13}CH_4$ = −47.16‰)[c]	116	−46.86 ± 0.2	+0.3 ± 0.2
Simulated transfer of CH_4 Std 2	8	−47.0 ± 0.3	+0.16 ± 0.3
Preanthropogenic air from Siple Dome ice core gas ages (1837–1907 A.D.)	10	−48.8 ± 0.3	N/A

[a]N/A denotes "not applicable."
[b]On the basis of CF-IRMS analyses of liquid CO_2 via primary gaseous CO_2 that was previously calibrated to VPDB via NIST SRM 8563 and 8564.
[c]Assigned $\delta^{13}CH_4$ value for the CH_4 air standards were provided by Stan Tyler (University of California, Irvine).

trap 2 at −130°C (pentane slush) where the CH_4 is trapped on a 0.32 cm × 10 cm SS column packed with 80/100 HaySep D material. The sample container is flushed for 1400 s to insure quantitative trapping of CH_4 in trap 2. Valco valves 1 and 2 are then switched so the CH_4 is transferred from trap 2 to trap 3, which contains a 1-m section of the 0.32-mm poraplot column immersed in the −130°C pentane bath. After 500 s, trap 3 is raised out of the pentane bath mobilizing the CH_4 that is then separated from other trace impurities in the remainder of the poraplot column before entering the oxidation furnace (Pt, Cu, and Ni wires at 1050°C) for quantitative conversion to CO_2. The effluent from the furnace passes through a 15-cm Nafion drying system cooled to −60°C for efficient water removal [*Leckrone and Hayes*, 1998]. The sample gas stream then enters the open split leading to the ion source of the mass spectrometer. The CO_2 peak is monitored with three separate faraday cups that record each isotope of CO_2 (m/e = 44,45 and 46). The area of each isotope peak was integrated before ratios of the peak areas were compared to CO_2 standard peaks that were introduced before and after the sample for reference.

[14] The $^{13}C/^{12}C$ of the CH_4 is referenced to a working standard of liquefied CO_2 that was previously calibrated to VPDB using NIST CO_2 reference standards (8563 and 8564). The $\delta^{13}CO_2$ of the working standard was −33.26 ± 0.07‰ (1σ, N = 16) based on periodic analyses of the working standard against a primary lecture bottle of gaseous CO_2. In all cases, the measured 45/44 ratios were corrected for ^{17}O following *Santrock et al.* [1985].

2.3. Ice Core Methodology for $\delta^{13}C$ of CH_4

[15] The analytical methodology for extracting and analyzing trapped gases in ice can be broken into two distinct parts: the liberation of the trapped gases from the ice core sample and the $\delta^{13}CH_4$ analysis. The extraction of the gases from the 1–1.5 kg ice core samples was accomplished using a "wet" extraction technique. The outside of the ice samples were initially shaved to remove the outermost ~5 mm of ice. The shaved samples were then inserted into a 7.6 cm × 35 cm stainless cylinder that was sealed with a copper gasket prior to evacuation. After 1 hour of evacuation, the cylinder was isolated and inserted into a warm water bath to melt the ice samples and liberate the trapped air into the headspace above the meltwater. The cylinder was then transferred to a large SS Dewar where the meltwater is refrozen using liquid nitrogen. After 30 min, the headspace was flushed with UHP He (60 cc/min) through a water trap (−110°C) and a HaySep D trap at −130°C where the CH_4 was quantitatively removed from the air. After 1 hour, the CH_4 trap was isolated and removed from the system. The trap was then connected to the PreCon and processed in an identical fashion as the air samples described above.

3. Data

3.1. PSU Procedure Verification

[16] Each stage of the analytical procedure was checked to quantify the degree to which the measured $\delta^{13}CH_4$ reflects the $\delta^{13}C$ of CH_4 in the original sample. To establish the integrity of the preconcentration/mass spectrometry, we analyzed 50–100 cc (STP) aliquots of two compressed air standards that had been previously calibrated by Stan Tyler (UCI) as part of their atmospheric $\delta^{13}CH_4$ program [*Rice et al.*, 2001; *Tyler et al.*, 1999]. The assigned $\delta^{13}CH_4$ values for the two standards (CH_4 Std 1 and 2 in Table 1) are −19.6 ± 0.03‰ and −47.16 ± 0.04‰, respectively. Aliquots of these compressed air standards are routinely expanded into numerous 50–100 cc flasks at the beginning of each day to insure the complete analytical protocol provides accurate and precise $\delta^{13}CH_4$ values. If the results on the daily standards are more than 0.2‰ away from the assigned value, system checks and additional standards are run until the results fall within the 0.2‰ tolerance. Over the 3-year period since we began measuring $\delta^{13}CH_4$, we have measured 51 aliquots of CH_4 Std 1 and 116 aliquots of CH_4 Std 2 yielding average values of −19.6 ± 0.3‰ and −46.86 ± 0.2‰, respectively (Table 1). The difference between the average values and the assigned values is less than 0.2‰, suggesting that our analytical procedures provide accurate $\delta^{13}CH_4$ data with an external precision of 0.2‰.

[17] Aliquots of CH_4 Std 2 air standards were processed through the entire ice core procedure using degassed ice from Siple Dome. We performed eight simulated trapped gas transfers between October 2002 and November 2003 using 100–150 cc (STP) aliquots of CH_4 Std 2 with an assigned $\delta^{13}CH_4$ value of −47.16‰ (Table 1). The resulting average $\delta^{13}CH_4$ was −47.0 ± 0.3‰. The results are indistinguishable from the assigned value, indicating that the complete procedure did not measurably alter the isotopic composition of CH_4. The standard deviation about the mean for the simulated transfers is ~0.1‰ higher than that based on replicate analyses of the standards expanded directly into glass flasks. We attribute the added uncertainty to variable amounts of water that get transferred to the PreCon with the fossil air sample. Small changes in the water background in the source accompanying the sample

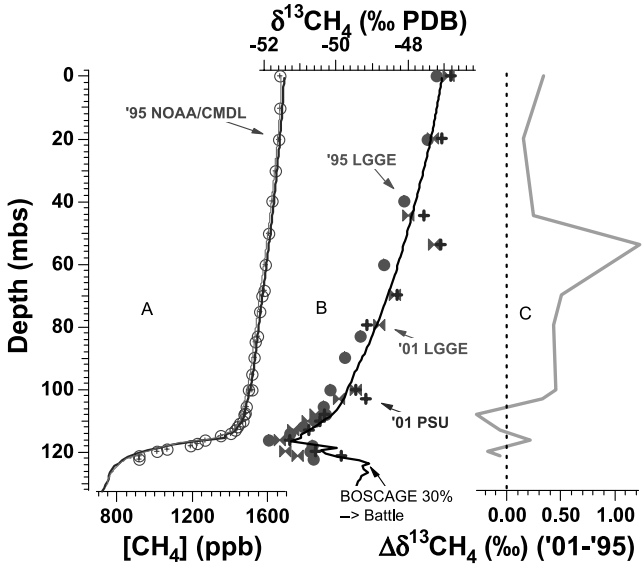

Figure 2. Results of CH_4 and $\delta^{13}CH_4$ analyses on South Pole Firn air. (a) CH_4 data were measured on the 1995 samples at NOAA/CMDL (P. Tans, personal communication, 2002). The red and blue lines are the model predicted CH_4 profiles from the *Battle et al.* [1996] (blue) and *Rommelaere et al.* [1997] (red) firn models. (b) The $\delta^{13}CH_4$ measurements at LGGE (red, 1995 and 2001) and PSU (blue, 2001 only). Also plotted with a solid black line is the inferred firn air $\delta^{13}CH_4$ profile (2001) using the BOSCAGE-8 atmospheric output with 30% of total biomass burning assigned to anthropogenic activities and the *Battle et al.* [1996] firn air model. (c) The $\Delta\delta^{13}CH_4$ data are the difference between the 2001 and 1995 LGGE data. See color version of this figure at back of this issue.

CO_2 influence the measured 45/44 ratio through protonation of CO_2 to HCO_2^+ (m/e = 45) in the ion source [*Leckrone and Hayes*, 1998].

3.2. South Pole Firn Air

[18] The NOAA/CMDL [CH_4] data show a gradually decreasing trend with depth to 114 m with a much steeper rate of decrease below 114 m to the final bubble close off at 122 m where the measured CH_4 was 910 ppb (Figure 2). The 114-m horizon represents the top of the lock-in zone below which exchange with the overlying firn is substantially restricted. The $\delta^{13}CH_4$ data show a gradually decreasing trend between the surface and 110 m. Between 110 m and 122 m, the $\delta^{13}CH_4$ values exhibit an interesting oscillation that has not previously been observed in firn air studies because of their younger firn air age. The minimum values approach −51.7‰ at 117 m with increasing $\delta^{13}CH_4$ values below 117 m. This oscillation is generated by the faster diffusion coefficient of $^{12}CH_4$ in air compared to $^{13}CH_4$, superimposed on a present-day atmospheric $\delta^{13}CH_4$ value which is comparatively heavier than the pre-industrial one.

[19] There are three firn air $\delta^{13}CH_4$ data sets from the South Pole plotted in Figure 2. Two of the three $\delta^{13}CH_4$ data sets were generated at LGGE, one on each of the two expeditions (1995 and 2001). At each depth, multiple flasks were collected to provide enough firn air for all analyses. All data plotted in Figure 2 are average results from all flasks that were measured at each depth by each lab (generally duplicate flasks with duplicate or triplicate analyses on each flask in each laboratory). The $\delta^{13}CH_4$ measurements were also made at PSU on the same 2001 flasks as an intercalibration exercise. These data, along with the corresponding LGGE data for each flask, are tabulated in Table 2. All data have been corrected for gravitational fractionation using the $\delta^{15}N$ of N_2 measured on each flask at Princeton (M. Bender, personal communication, 2002). Eleven flasks were measured at PSU before shipping 20 flasks to LGGE for analyses. Five of those flasks were remeasured at PSU after the LGGE analyses to check for alterations associated with the trans-Atlantic shipments and the LGGE analyses. The average difference between the PSU analyses performed before and after the LGGE analyses was −0.05‰, indicating no measurable change in the $\delta^{13}CH_4$ values.

[20] Comparison of the $\delta^{13}CH_4$ results from each flask measured at LGGE and PSU showed the average difference between the 19 flasks was 0.32 ± 0.28‰. This value is comparable to the external precision associated with replicate analyses on a given flask (∼0.1‰). We interpret this close agreement as indicating the analytical procedures and working standards at the two laboratories are consistent within our external precision.

[21] In order to compute the net change in the $\delta^{13}CH_4$ between the two firn air expeditions (2001 − 1995 = $\Delta\delta^{13}CH_4$), we interpolated the 1995 $\delta^{13}CH_4$ profile at depths for which samples were taken during the 2001 expedition. We then used the average LGGE data at each depth for the two samplings to calculate the difference ($\Delta\delta^{13}CH_4$, Figure 2). With the exception of the 53 mbs sample, the upper 100 m showed the 2001 values to be ∼0.3‰ higher than the 1995 values. The $\delta^{13}CH_4$ values below 100 mbs are effectively identical given our sample resolution. This was expected as the air in the deeper portions of the firn has not communicated with the overlying atmosphere during the 6 years that separate the two expeditions. We interpret this close agreement below 100 mbs as evidence that the sampling and analytical techniques employed during the two expeditions are indistinguishable from one another.

3.3. Siple Dome Ice

[22] We have analyzed 10 individual samples of ice from a shallow Siple Dome ice core that was drilled during the 1996/1997 field season (81°24.18′S, 148°18.14′W, elevation = 621 masl, mean annual temp = −25.4°C, accumulation ∼11 cm ice/yr [*Taylor et al.*, 2004]). The depths ranged from 62.4 m to 70.6 m, with corresponding gas ages between 1837 and 1907 A.D. The average $\delta^{13}CH_4$ was −48.8 ± 0.37‰ (1σ). This value has been corrected for gravity with three measurements of the $\sigma^{15}N$ of N_2 ($\delta^{15}N_2$ = 0.22 ± 0.02‰) (1σ) using a previously described technique [*Sowers et al.*, 1989; *Sowers and Jubenville*, 2000]. One sample from 66.5 mbs (gas age = 1873 A.D.) provided a $\delta^{13}CH_4$ value of −49.8‰. While we cannot attribute the anomalous result to any identified artifact associated with

Table 2. LGGE and PSU $\delta^{13}CH_4$ Data From the 2001 Expedition

Flask ID	Depth, mbs	$\delta^{15}N_2$,[a] ‰ Atm N_2	PSU $\delta^{13}CH_4$, ‰ PDB	LGGE $\delta^{13}CH_4$, ‰ PDB	Corr. LGGE $\delta^{13}CH_4$,[b] ‰ PDB	PSU−LGGE, ‰
775	0	−0.001	−46.84 ± 0.15	−46.67	−46.87 ± 0.12	0.04
SDF-49	19.99	0.107	−46.98 ± 0.02	−47.01	−47.32 ± 0.18	0.34
SDF-27	19.99	0.102	−47.14 ± 0.06	−47.03	−47.34 ± 0.14	0.20
523	44.47	0.242	−47.57 ± 0.06	−47.55	−48.00 ± 0.17	0.43
O_2/CO_2 8	53.61	0.260	−47.09 ± 0.04	−46.81	−47.28 ± 0.19	0.19
SP-335	69.61	0.338	−48.30 ± 0.01	−47.83	−48.38 ± 0.07	0.07
SP-141	69.61	0.354	−48.30 ± 0.17	−47.96	−48.53 ± 0.14	0.22
TF-23	79.4	0.412	−48.61 ± 0.08	−48.19	−48.81 ± 0.11	0.20
818	100.16	0.536	−49.15 ± 0.11	−48.72	−49.46 ± 0.20	0.32
SP-64	100.2	0.555	−49.77 ± 0.08	−49.17	−49.94 ± 0.21	0.16
SP-2	102.8	0.538	−49.18 ± 0.01	−49.17	−49.92 ± 0.21	0.74
SP-20	108	0.581	−50.32 ± 0.05	−49.78	−50.57 ± 0.10	0.25
SP-37	110	0.626	−50.27 ± 0.06	−49.95	−50.79 ± 0.41	0.52
SP-38	110	0.610	−50.65 ± 0.08	−49.89	−50.71 ± 0.08	0.07
SP-45	113.1	0.624	−50.75 ± 0.18	−50.34	−51.17 ± 0.12	0.42
TF-40	116.2	0.598	−51.27 ± 0.01	−50.75	−51.56 ± 0.03	0.29
668	119.87	0.611		−50.57	−51.39 ± 0.13	
SP-43	119.9	0.621	−50.56 ± 0.01	−49.55	−50.38 ± 0.13	−0.17
O_2/CO_2 4	121.3	0.619	−50.05 ± 0.03	−50.22	−51.05 ± 0.22	1.00
O_2/CO_2 6	121.3	0.649	−49.66 ± 0.16	−49.55	−50.41 ± 0.13	0.75
Average					PSU-LGGE	0.32 ± 0.28

[a]The $\delta^{15}N_2$ of N_2 measurements were made by M. Bender at Princeton and are reported with respect to atmospheric N_2.
[b]LGGE $\delta^{13}CH_4$ were corrected for an additional 0.21‰ shift that was related to a change in the primary liquid CO_2 reference tank value.

the extraction, we consider this value questionable given that it falls more than 1‰ below the average of the other nine samples (−48.7 ± 0.1‰). We consider the average of the nine samples (−48.7 ± 0.1‰) to be the best estimate of the average $\delta^{13}CH_4$ for the later part of the nineteenth century.

4. Firn Air Modeling

[23] In order to extract the atmospheric history of $\delta^{13}CH_4$ from our firn air measurements, we have employed two 1-D gas diffusion models that account for the main factors influencing the firn air composition. The upper few meters of firn are advectively mixed with the overlying atmosphere by barometric fluctuations and wind pumping. Below this convective zone, air mixes solely by diffusion in an isothermal environment where gravitational fractionation occurs down to the top of the "lock-in" zone. Within the lock-in zone, air cannot communicate with the overlying firn air/atmosphere so no additional gravitational fractionation occurs. Finally, as bubbles are pinched off, a small amount of air is forced upward because bubbles are closing off in a region of increasing hydrostatic load.

[24] The two key features of a firn air model are the effective diffusivity and the open porosity profiles. For both models, temperature, accumulation rate, and firn structural parameters are held constant for the duration of the simulations. *Battle et al.* [1996] developed records of open porosity based on the measured density profile following *Schwander et al.* [1988]. The effective diffusivity for CO_2 was initially based on the open porosity following *Schwander et al.* [1988]. The CO_2 diffusivity profile was subsequently tuned until the model CO_2 profile matched the measured profile using the Law Dome CO_2 record as the atmospheric CO_2 forcing function. Once the CO_2 effective diffusivity was established, other trace gas species can be modeled in a forward sense using the ratio of their molecular diffusivities relative to CO_2 [*Trudinger et al.*, 1997].

[25] Additionally, we adapted an air transport model developed by *Rommelaere et al.* [1997] for the South Pole. For this model, we developed an open porosity versus depth profile for South Pole following *Goujon and Barnola* [2003] using total gas content measurements from *Martinerie et al.* [1995]. The effective diffusivity profile was established by inverting the measured CO_2 versus depth profile using the atmospheric CO_2 record from *Etheridge et al.* [1996] as the true atmospheric record. Once the effective CO_2 diffusivity profile was established, other species were modeled in a forward sense after calculating individual molecular diffusion coefficients (D_i) relative to CO_2 following [*Bzowski and Kestin*, 1990]

$$\frac{D_i}{D_1} = \sqrt{\frac{M_1(M_i + M_{air})}{M_i(M_1 + M_{air})}}, \quad (1)$$

where

M_1 gram molecular weight of CO_2 (0.044 kg/mole);
M_i gram molecular weight of each CH_4 isotopomer (i);
$^{12}CH_4$ = 0.01604 kg/mole;
$^{13}CH_4$ = 0.01704 kg/mole;
M_{air} gram molecular weight of air (0.028966 kg/mole);
D_1 CO_2 diffusivity in air at the South Pole (1.07 m^2/day);

The diffusion coefficients for $^{12}CH_4$ and $^{13}CH_4$ were 1.471 m^2/d and 1.444 m^2/d, respectively, after accounting for the lower atmospheric pressure at South Pole.

[26] In order to validate the diffusivity profile deduced from CO_2 measurements, we utilized the well-known

atmospheric CH_4 record from Law Dome. We constructed an atmospheric methane record for the past 300 years using ice core measurements from DE08 and DSS ice cores from 1700 to 1978 A.D. [*Etheridge et al.*, 1998], atmospheric measurements at Cape Grim from 1978 to 1983 [*Langenfields and Fraser*, 1996], and direct atmospheric measurements at South Pole between 1983 and the date we recovered the firn air [*Dlugokencky et al.*, 1994, 1998] (NOAA/CMDL, ftp://ftp.cmdl.noaa.gov/ccg/ch4/flask/month/spomm.ch4). This atmospheric record was run through both the Battle and LGGE firn models with the resulting CH_4 profiles plotted in Figure 2 along with the measured values in 1995. The agreement between the firn CH_4 data and the model reconstructions is good, as seen in Figure 2, thus validating the open porosity and diffusivity profiles used in the model. The average difference between the two model CH_4 profiles is 11 ± 10 ppb. The depth-averaged differences between the measured and modeled CH_4 data are 22 ± 30 ppb and 11 ± 36 ppb for the LGGE and Battle models, respectively. We interpret the strong similarity between the measured and modeled CH_4 profiles as evidence that (1) the parameterizations of the physical nature of gas mixing and trapping in the two models are virtually identical, and (2) the models capture the important factors controlling gas movement in the firn.

[27] Although routinely used for mixing ratios, the implementation of the inverse technique developed by *Rommelaere et al.* [1997] for isotope ratios has been hampered by the nonlinearities associated with modeling two isotopes simultaneously. In order to construct atmospheric $\delta^{13}CH_4$ records that were consistent with our firn air $\delta^{13}CH_4$ data, we utilized a Monte Carlo approach with a wide range of hypothetical atmospheric $\delta^{13}CH_4$ histories that were tested using the forward firn air model. The input scenarios were parameterized as third-order polynomial functions that provide acceptable trends of CH_4 isotopic ratios (obviously, for example, low-frequency sinusoidal functions would not be compatible with our knowledge of trace gas trends and their budgets). The validity of each tested scenario, through the agreement between the modeled and experimental firn profiles, is evaluated with a chi test [*Aballain*, 2002]. Scenarios are accepted when the difference between modeled and experimental data is less than 0.6‰ (that is, $\chi^2 \leq 0.36$).

[28] The maximum and minimum atmospheric $\delta^{13}CH_4$ values from the Monte Carlo simulations are plotted in Figure 3. The color coding for the lines represents the percent of air of a specific age that is represented in the South Pole firn. For example, ~25% of air from 1900 A.D. still resides in the firn with the balance (75%) either mixed out of the firn or trapped in bubbles below. The lower percentage values are located just above the bubble close-off region and the highest percentages are located at the surface. This information is important in assessing the degree to which the Monte Carlo results can be applied to paleoatmospheric reconstructions. As the percent of fossil surface air that is represented in the firn goes down, so does our confidence in the inferred paleoatmospheric $\delta^{13}CH_4$ from the firn air analyses. Thus we are less confident in the paleoatmospheric reconstructions before ~1900 A.D. based on firn air data alone.

5. Discussion

5.1. Evolution of $\delta^{13}CH_4$ Between 1995 and 2001 at the South Pole

[29] One advantage of performing multiple firn air experiments at the same locale is the fact that seasonal variations in surface air are smoothed out in the firn by diffusion. Resampling firn air thereby provides a unique means of deciphering the compositional changes without having to continually sample and measure air from a site. In this case, we sampled the interstitial firn air at South Pole in January of 1995 and again in January of 2001, providing a 6-year integrated window.

[30] To determine the net change in $\delta^{13}CH_4$, we utilized the 1995 and 2001 $\delta^{13}CH_4$ data generated at LGGE (Figure 2b). To calculate the $\delta^{13}CH_4$ difference, we interpolated the 1995 profile at depths sampled in 2001. The resulting $\Delta\delta^{13}CH_4$ profile is plotted in Figure 2c. Discounting the anomalous 2001 sample at 53 mbs, the average $\Delta\delta^{13}CH_4$ between 20 and 103 m is 0.56 ± 0.14‰ ($N = 6$). This value should represent the true $\delta^{13}CH_4$ change over the 6-year period as it was determined by measurements made in the same laboratory using identical equipment and procedures. However, we have documented a measurable offset between the CSIRO air standard cylinder measurements that were made during the two analytical windows. For the 1995 suite, 43 measurements of the CSIRO standard were made with a mean $\delta^{13}CH_4$ value of −47.22 ± 0.08‰. This value is 0.21‰ lower than the corresponding $\delta^{13}CH_4$ value obtained from the same tank in 2001 (−47.01 ± 0.012‰, $N = 25$). We attribute the different results to slightly higher water background levels associated with the 2001 samples [*Leckrone and Hayes*, 1998], and a drift in the $\delta^{13}C$ value of the liquid CO_2 tank that served as the working reference. We have thus applied the 0.21‰ correction to all 2001 LGGE $\delta^{13}CH_4$ values (Table 2). Applying this difference to the measured $\Delta\delta^{13}CH_4$ values, we calculate that the net change in atmospheric $\delta^{13}CH_4$ over the 6-year period was 0.35 ± 0.2‰. This value translates to +0.06 ± 0.03‰/yr for our best estimate of the average annual $\delta^{13}CH_4$ change recorded in the firn at South Pole. This value is slightly higher than that determined by *Bräunlich et al.* [2001] and *Francey et al.* [1999] of +0.04 ± 0.01‰/yr for the last 2 decades of the twentieth century. The increasing $\delta^{13}CH_4$ trend is thought to be the combined result of an increase in the proportion of $\Delta\delta^{13}CH_4$ emissions with elevated $^{13}C/^{12}C$ values and/or simply the added time needed for atmospheric $\delta^{13}CH_4$ to adjust to a change in sources/sinks [*Tans*, 1997].

5.2. Preliminary Tests With an Atmospheric Isotope Model

[31] The twentieth century $\delta^{13}CH_4$ record from the South Pole firn air provides additional constraints on the cause of the 150% mixing ratio increase. Given the plethora of sources, sinks, and their characteristic isotope fingerprints, it is not possible to derive a single set of historical emission

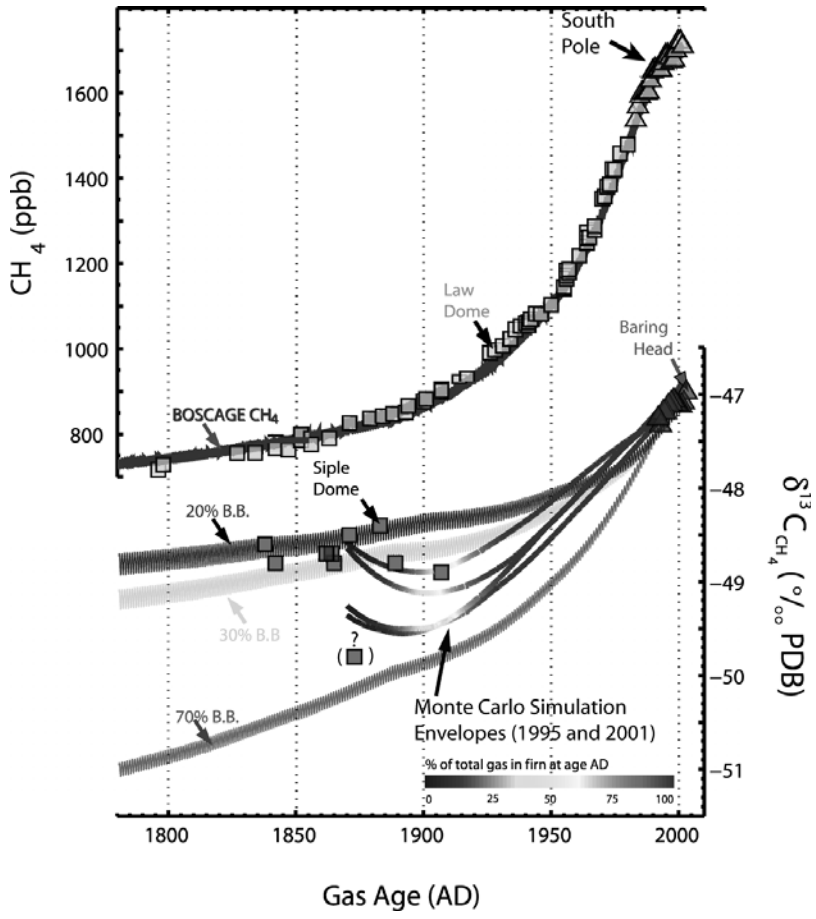

Figure 3. Records of $[CH_4]$ and $\delta^{13}CH_4$ covering the last 2 centuries: (top) $[CH_4]$ data from *Etheridge et al.* [1998] along with the resulting BOSCAGE predicted curve, and (bottom) model records of $\delta^{13}CH_4$ versus time, ice core data from Siple Dome, and direct atmospheric measurements from Baring Head [*Lowe et al.*, 1994]. Maximum and minimum curves of the Monte Carlo simulations are plotted with color lines. The color coding corresponds to the percent of air in the firn that is represented at the corresponding historical date. One Siple Dome $\delta^{13}CH_4$ value from 66.5 mbs (1873 A.D.) is considered questionable as it was 1‰ lower than the other nine samples. Also plotted are three BOSCAGE simulations with varying percentages of biomass burning CH_4 attributed to anthropogenic activities. The model simulations with 20–30% of biomass burning attributed to anthropogenic activities is in agreement with the Siple Dome and Monte Carlo simulation from South Pole firn air. See color version of this figure at back of this issue.

records that will satisfy the $\delta^{13}CH_4$ data. To address this problem, we utilized an eight-box atmospheric CH_4 model (BOSCAGE-8) that was constructed for performing long-term sensitivity tests of various emission scenarios [*Marik*, 1998]. Briefly, the BOSCAGE-8 model consists of eight boxes: six boxes cover the troposphere in 30° meridional bands and two for each hemisphere of the stratosphere with the boundary between the troposphere and stratosphere set at 200 hPa. Model dynamics were tuned with SF_6 following *Levin and Hesshaimer* [1996]. The model is based on seasonal and latitudinal variations in the emission and sink terms as well as the tabulated characteristic isotopic values adopted from the inverse modeling of *Hein et al.* [1997]. Starting with an initial inventory of sources and their distribution (Table 3), the model calculates the mixing and isotopic ratios inside each box taking into account the exchange times and the methane lifetime (about 8 years) estimated from the sinks. The free parameters of the model are the strengths of each source and sink and the characteristic isotope value of each source group (animals, rice, bogs, swamps, landfills, biomass burning, coal, oil/gas). In order to reproduce the industrial increase of CH_4 mixing ratio, *Marik* [1998] keeps the natural sources constant and sets the anthropogenic sources (animals, rice, landfills, coal, oil/gas, and part of the total biomass burning) proportional to human population, as suggested by *Khalil and Rasmussen* [1985]. The BOSCAGE-8 model does not have a chemical module to predict changes in [OH] that result from increased CH_4 and CO loadings. To account for the decreasing [OH] levels, we adopt a 25% linear decrease between 1885 A.D. and the present that was suggested by *Marik* [1998] in line with results from *Khalil and Rasmussen* [1985]. Model runs with these settings compared extremely

Table 3. BOSCAGE-8 Base Scenario of CH_4 Sources and Their Characteristic $\delta^{13}CH_4$ Values for the Period 1985 A.D.[a]

Source	Amount, Tg/yr	$\delta^{13}CH_4$, ‰ PDB	δD_{CH4}, ‰ SMOW	Box 1 90°S–60°S, %	Box 2 60°S–30°S, %	Box 3 30°S–0°, %	Box 4 0°–30°N, %	Box 5 30°N–60°N, %	Box 6 60°N–90°N, %
1985 Sources									
Animals	84.1	−61.5 ± 2.9	−330	0	4.94	18.73	41.13	35.20	0.0
Rice	71.9	−62.5 ± 2.8	−335	0	0.18	13.9	77.50	8.42	0.0
Bogs	56.1	−62.9 ± 2.7	−350	0	0.18	5.25	5.75	64.79	24.03
Swamps	141.3	−62.6 ± 3.3	−330	0	2.9	50.19	38.36	8.21	0.35
Landfills	23.1	−50.7 ± 2.0	−280	0	0.25	1.95	16.35	80.83	0.62
Biomass	53.2	−25.8 ± 2.9	−40	0	0.2	55.95	43.85	0.0	0.0
Coal	39.8	−34.3 ± 2.9	−180	0	0.0	9.95	25.93	61.02	3.10
Oil gas	47.1	−39.6 ± 2.0	−190	0	0.72	8.22	40.70	50.36	0.0
Siberian gas	10.0	−39.9 ± 2.0	−205	0	0.0	0.0	0.0	58.33	41.67
Percent	100 (527)	−53.5	−263	0%	1.7%	26.14%	38%	29.7%	3.7%
FW$\delta^{13}CH_4$,[b] ‰		−53.5		0	−60.7	−53.0	−54.4	−52.2	−56.1
FW δD_{CH4},[b] ‰			−263	0	−321	−260	−277	−279	−307
1985 Sinks									
OH[c]	−432	1.0054[d]	1.345	0.0079	0.0382	0.162	0.179	0.078	0.02
Soils[e]	−33	1.024[d]	1.024	0	0.01	0.272	0.303	0.35	0.06
Strat.(OH+Cl)	−35	1.016[d]	1.161						

[a]The source/sink distribution for each box was determined from an adaptation of the *Hein et al.* [1997] 3-D inversion to the 2-D construct of BOSCAGE-8. Characteristic $\delta^{13}C$ and δD_{CH4} values were taken from the literature as stipulated by *Hein et al.* [1997] and *Marik* [1998].

[b]FW represents the flux-weighted isotope value for each atmospheric box. The value is determined by multiplying each individual source delta value by the percent in the latitude box and then averaging all the sources.

[c]CH_4 loss via OH and Cl in each box is reported as in terms of the lifetime of CH_4 in each box. Units are yr^{-1}. For the two stratospheric boxes (7 and 8), the corresponding values are 0.046 yr^{-1} and 0.039 yr^{-1}.

[d]The isotope effect of each sink term is reported as an isotope fractionation factor (α) with respect to the CH_4 in each box. For tropospheric OH, α_{OH} = 1.0054 is taken from *Cantrell et al.* [1990]. α_{soils}, and $\alpha_{stratosphere}$ (including stratospheric Cl) are model tuned parameters which are very close to literature values (α_{soils} = 1.021 ± 0.005 [*King et al.*, 1989]), and ($\alpha_{stratosphere}$ = 1.0154 ± 0.008, [*Rice et al.*, 2003]).

[e]The latitudinal distribution of soil uptake was adopted from *Dörr et al.* [1993] and is reported as a percentage of the total emissions (33 Tg/yr) in each box.

well with direct measurements of $[CH_4]$, $\delta^{13}CH_4$, and δD_{CH4} during the 1990s from three sites: Alert (82°N), Izana (28°N), and Neumayer Station (70°S) [*Marik*, 1998].

5.3. Sensitivity Tests With the BOSCAGE-8 Model

[32] There are effectively two bacterial processes that liberate methane. In terrestrial ecosystems, acetate fermentation is the dominant pathway whereby methanogenic bacteria produce methane with characteristic $\delta^{13}CH_4$ values between −55 and −65‰ [*Francey et al.*, 1999; *Quay et al.*, 1999, 1991; *Whiticar*, 2000, 1993]. In deep sea marine sediments, CO_2 reduction is the primary pathway yielding $\delta^{13}CH_4$ values between −55 and −70‰ [*Whiticar et al.*, 1986]. The large $\delta^{13}CH_4$ overlap between these two metabolic pathways makes it difficult to ascribe a given change in the atmospheric $\delta^{13}CH_4$ to any particular source. However, CH_4 associated with biomass burning has a distinct $\delta^{13}CH_4$ value (−27 ± 3‰ [*Quay et al.*, 1991]) relative to the dominant bacterial sources. Thus, while we cannot rule out changes in the characteristic $\delta^{13}CH_4$ value for any of the anthropogenically mediated sources that would account for the increasing $\delta^{13}CH_4$ values we recorded over the past 150 years, we suggest that the more likely explanation for the increasing $\delta^{13}CH_4$ values is increased CH_4 emissions from biomass burning. To assess the magnitude of the expected increase in biomass burning that would account for the $\delta^{13}CH_4$ increase, we performed three sensitivity tests involving changes in the percentage of total biomass burning CH_4 that is associated with anthropogenic activities.

[33] The optimum scenario from *Marik* [1998] identified 30% of the total biomass burning CH_4 as being anthropogenic in origin. In our first scenario, we assumed that 70% of the 53.2 Tg/yr of biomass burning methane in 1985 was related to anthropogenic activities. Two other runs were made in which we assigned the anthropogenic contribution as 20% and 30% of total. In all runs, the natural emissions were held constant for the duration of the model run. To maintain the atmospheric loading for all three runs, the OH sink term during the nineteenth century had to be increased by 40%, 35%, and 25% relative to today's value for the simulations in which anthropogenic biomass burning accounted for 20%, 30%, and 70% of the total.

[34] The three corresponding $\delta^{13}CH_4$ trends calculated with the BOSCAGE-8 model for the southern tropospheric box since 1790 A.D. are shown in Figure 3. The output from the BOSCAGE-8 scenarios with 20 and 30% of total biomass burning attributable to anthropogenic activities envelopes both the 1995 A.D. and 2001 A.D. Monte Carlo envelopes as well as the Siple Dome $\delta^{13}CH_4$ results. One interpretation of these results holds that between 20% (11 Tg/yr) and 30% (16 Tg/yr) of total CH_4 from biomass burning in 1985 AD is attributable to anthropogenic activities. It is, however, noteworthy that this result assumes (1) no anthropogenic biomass burning emissions at 1800 A.D. whereas savanna burning and

wood use for cooking and heating were already significant contributors, and (2) that all natural CH_4 emissions have remained constant and the characteristic $\delta^{13}CH_4$ values that we have assigned to the various sources and sinks (Table 3) have also remained constant (thus assuming no shift of the anthropogenic biomass burning signature from "heavy" savanna burning to "lighter" forest burning).

[35] We finally utilized the $\delta^{13}CH_4$ output from the BOSCAGE-8 model as the input for the forward firn model to compare the predicted firn $\delta^{13}CH_4$ profile with our measurements. This test effectively evaluates the internal consistency between the BOSCAGE model assumptions and the most accurate estimates of the atmospheric $\delta^{13}CH_4$ record over the last century. We utilized the BOSCAGE model output that resulted from assuming that 30% of total biomass burning CH_4 emissions were anthropogenically produced. This BOSCAGE atmospheric record was used as the surface forcing along with the CH_4 loading record from *Etheridge et al.* [1998] in the Battle model ending in January 2001. The resulting $\delta^{13}CH_4$ profile is plotted in Figure 2b (black line). The difference between the BOSCAGE predicted $\delta^{13}CH_4$ profile and the measured data (omitting the 53 mbs sample) is 0.08‰ with the upper portion of the model curve having slightly lower $\delta^{13}CH_4$ values and the lower portion of the model curve having slightly higher $\delta^{13}CH_4$ values relative to the measured values. Overall, we consider the close agreement between the BOSCAGE model profile and the measured profile as support for the atmospheric $\delta^{13}CH_4$ history resulting from the chosen scenario.

[36] The BOSCAGE-8 model does not include a separate term for methane decomposition by stratospheric Cl. Rather, we have modeled the stratospheric uptake via both OH and Cl with a single fractionation factor (α_{strato} = 1.16). This tuned parameter is very close to the empirically determined value (α_{strato} = 1.153 ± 0.008) from *Rice et al.* [2003]. As the stratospheric fractionation factor is held constant throughout the model run and stratospheric Cl levels must have been lower during the eighteenth and nineteenth centuries, the model predicted tropospheric $\delta^{13}CH_4$ values during the nineteenth century are slightly higher than model runs in which the Cl effect had been treated separately. The magnitude of this oversimplification must be less than the total effect attributable to Cl today (0.2–0.5‰) [*McCarthy et al.*, 2003; *Platt et al.*, 2004; *Wang et al.*, 2002].

[37] These preliminary tests using our reconstructed $\delta^{13}CH_4$ trends thus suggest that a significant contribution of natural biomass burning to the CH_4 budget must be invoked for the last 2 centuries. Our results also suggest that the source/sink scenario developed by *Marik* [1998] is compatible with our $\delta^{13}CH_4$ data over the last century. Testing other scenarios was beyond the scope of our study and will motivate future research.

6. Conclusions

[38] We have reconstructed a record of $\delta^{13}CH_4$ over the past 2 centuries (nineteenth and twentieth) from a Siple Dome shallow ice core and two separate firn air samplings at the South Pole. Our results suggest the $\delta^{13}CH_4$ was −48.8 ± 0.2‰ in the early 1800s and has increased exponentially to present-day values of −47.0‰ in 2001 A.D. The 1.8‰ $\delta^{13}CH_4$ change must be related to an increase in the proportion of CH_4 emissions with elevated $^{13}C/^{12}C$ ratios.

[39] In order to evaluate the reconstructed $\delta^{13}CH_4$ record in terms of historical emissions, we applied an eight-box atmospheric model (BOSCAGE) that accounts for meridional transport and cross-tropopause mixing in addition to a prescribed OH sink distribution. The inputs for the model are the time-dependent anthropogenic CH_4 emissions (tied to world population) and their assigned $\delta^{13}CH_4$ value. One scenario that is in agreement with our isotope data invokes an increase in biomass burning CH_4 emissions from 37 to 53 Tg/yr over the last 2 centuries. For this scenario, we maintained natural biomass burning values at 37 Tg/yr throughout the simulation and held the isotopic composition of all sources and sinks constant. Increased emissions throughout all simulations were tied to world population. It is important to note that this scenario is one of many possible solutions that are consistent with our $\delta^{13}CH_4$ record combined with the atmospheric loading record from *Etheridge et al.* [1998]. We expect to be able to add additional constraints to this problem with future D/H measurements of CH_4 trapped in ice.

[40] Finally, we sampled firn air from the South Pole station in 1995 and again in 2001 to establish the net change in $\delta^{13}CH_4$ over a 6-year period. Because the seasonal $\delta^{13}CH_4$ signal is damped within the firn, periodic measurements at a single firn site provide an ideal means of determining the average $\delta^{13}CH_4$ change over multiple years. Over the 6 years separating the two samplings (1995 and 2001), we measured a change of 0.35 ± 0.2‰. This implies the average annual increase in $\delta^{13}CH_4$ was 0.06 ± 0.03‰. This value is slightly higher than previous firn air estimates (0.04‰/yr) from single firn air reconstructions at Law Dome, Dronning Maud Land, and Dome C [*Bräunlich et al.*, 2001; *Francey et al.*, 1999].

[41] **Acknowledgments.** This research was supported by the NSF (OPP 95-26556, OPP 01-25981, and ATM-0117291 to TAS) and the National Institute of Global Environmental Change (NIGEC). It is a contribution to the European Commission project CRYOSTAT (EVK2-CT2001-00116) funded under the Energy, Environment and Sustainable Development Programme, 1998–2002. Additional support was provided by the French national program ECLIPSE. We thank Ingeborg Levin for providing access to the BOSCAGE model and Dave Scerbo for analytical support. We also thank P. Tans (NOAA/CMDL) for his continued support of the U.S. firn air program.

References

Aballain, O. (2002), Reconstruction de l'évolution passée du rapport isotopique $^{13}C/^{12}C$ du méthane atmosphérique, à partir de l'analyse de l'air extrait du névé polaire, Ph.D. thesis, Univ. Joseph Fourier, Grenoble, France.

Battle, M., et al. (1996), Histories of atmospheric gases from the firn at South Pole, *Nature*, *383*, 231–235.

Bräunlich, M., O. Aballain, T. Marik, P. Jöckel, C. A. M. Brenninkmeijer, J. Chappellaz, J.-M. Barnola, R. Mulvaney, and W. T. Sturges (2001), Changes in the global atmospheric methane budget over the last decades inferred from ^{13}C and D isotopic analysis of Antarctic firn air, *J. Geophys. Res.*, *106*(D17), 20,465–20,481.

Bzowski, J., and J. Kestin (1990), Equilibrium and transport properties of gas mixtures at low density: Eleven polyatomic gases and five noble gases, *J. Phys. Chem. Ref. Data*, *19*(5), 1179–1232.

Cantrell, C. A., R. E. Shetter, A. H. McDaniel, J. G. Calvert, J. A. Davidson, D. C. Lowe, S. C. Tyler, R. J. Cicerone, and J. P. Greenberg (1990), Carbon kinetic isotope effect in the oxidation of methane by the hydroxyl radical, *J. Geophys. Res.*, *95*(D13), 22,455–22,462.

Craig, H., C. C. Chou, J. A. Welhan, C. M. Stevens, and A. Engelkemeir (1988), The isotopic composition of methane in polar ice cores, *Science*, *242*, 1535–1539.

Dlugokencky, E. J., K. A. Masarie, P. M. Lang, P. P. Tans, L. P. Steele, and E. G. Nisbet (1994), A dramatic decrease in the growth rate of atmospheric methane in the Northern Hemisphere during 1992, *Geophys. Res. Lett.*, *21*(1), 45–48.

Dlugokencky, E. J., K. A. Masarie, P. M. Lang, and P. P. Tans (1998), Continuing decline in the growth rate of the atmospheric methane burden, *Nature*, *393*, 447–450.

Dörr, H., L. Katruff, and I. Levin (1993), Soil texture parameterization of the methane uptake in aerated soils, *Chemosphere*, *26*(1–4), 709–725.

Etheridge, D. M., L. P. Steele, R. L. Langenfields, R. J. Francey, J.-M. Barnola, and V. I. Morgan (1996), Natural and anthropogenic changes in atmospheric CO_2 over the last 1000 years from air in Antarctic ice and firn, *J. Geophys. Res.*, *101*(D2), 4115–4128.

Etheridge, D. M., L. P. Steele, R. J. Francey, and R. L. Langenfields (1998), Atmospheric methane between 1000 A. D. and present: Evidence of anthropogenic emissions and climatic variability, *J. Geophys. Res.*, *103*(D13), 15,979–15,993.

Flocke, F., et al. (1999), An examination of chemistry and transport processes in the tropical lower stratosphere using observation of long-lived and short lived compounds obtained during STRAT and POLARIS, *J. Geophys. Res.*, *104*(D21), 26,625–26,642.

Francey, R. J., M. R. Manning, C. E. Allison, S. A. Coram, D. M. Etheridge, R. L. Langenfelds, D. C. Lowe, and L. P. Steele (1999), A history of $\delta^{13}C$ in atmospheric CH_4 from the Cape Grim air archive and Antarctic firn air, *J. Geophys. Res.*, *104*(D19), 23,631–23,643.

Goujon, C., and J.-M. Barnola (2003), Modeling the densification of polar firn including heat diffusion: Application to close-off characteristics and gas isotopic fractionation for Antarctica and Greenland sites, *J. Geophys. Res.*, *108*(D24), 4792, doi:10.1029/2002JD003319.

Gupta, M., S. Tyler, and R. Cicerone (1996), Modeling atmospheric $\delta^{13}CH_4$ and the causes of the recent changes in atmospheric CH_4 amounts, *J. Geophys. Res.*, *101*(D17), 22,923–22,932.

Hansen, J., M. Sato, R. Ruedy, L. Andrew, and V. Oinas (2000), Global warming in the twenty-first century: An alternative scenario, *Proc. Natl. Acad. Sci.*, *97*(18), 9875–9880.

Hein, R., P. J. Crutzen, and M. Heimann (1997), An inverse modeling approach to investigate the global atmospheric methane cycle, *Global Biogeochem. Cycles*, *11*, 43–76.

Khalil, M. A. K., and R. A. Rasmussen (1985), Causes of increasing atmospheric methane: Depletion of hydroxyl radicals and the rise of emissions, *Atmos. Environ.*, *19*(3), 387–407.

King, S. L., P. D. Quay, and J. M. Lansdown (1989), The $^{13}C/^{12}C$ kinetic isotope effect for soil oxidation of methane at ambient atmospheric concentrations, *J. Geophys. Res.*, *94*(D15), 18,273–18,277.

Langenfields, R. L., and P. J. Fraser (1996), The Cape Grim Air Archive: The first seventeen years, in *Baseline Atmospheric Program Australia, 1994–1995*, pp. 53–70, Bur. of Meteorol., Melbourne, Victoria, Australia.

Leckrone, K. J., and J. M. Hayes (1998), Water-induced errors in continuous flow carbon isotope ratio mass spectrometry, *Anal. Chem.*, *70*, 2737–2744.

Levin, I., and V. Hesshaimer (1996), Refining of atmospheric transport model entries by the globally observed passive tracer distributions of ^{85}Kr and sulfur hexafluoride (SF_6), *J. Geophys. Res.*, *101*(D11), 16,745–16,755.

Lowe, D., C. A. M. Brenninkmeijer, G. W. Brailsford, K. R. Lassey, A. J. Gomez, and E. G. Nisbet (1994), Concentration and ^{13}C records of atmospheric methane in New Zealand and Antarctica: Evidence for changes in methane sources, *J. Geophys. Res.*, *99*(D8), 16,913–16,925.

Lowe, D., et al. (1999), Shipboard determinations of the distribution of ^{13}C in atmospheric methane in the Pacific, *J. Geophys. Res.*, *104*(D21), 26,125–26,135.

Marik, T. (1998), Atmospheric $\delta^{13}C$ and δD measurements to balance the global methane budget, Ph.D. thesis, Ruprecht-Karls-Univ., Heidelberg, Germany.

Martinerie, P., G. P. Brasseur, and C. Granier (1995), The chemical composition of ancient atmospheres: A model study constrained by ice core data, *J. Geophys. Res.*, *100*(D7), 14,291–14,304.

McCarthy, M. C., K. A. Boering, A. Rice, S. Tyler, P. Connell, and E. Atlas (2003), Carbon and hydrogen isotopic composition of stratospheric methane: 2. Two-dimensional model results and implication for kinetic isotope effects, *J. Geophys. Res.*, *108*(D15), 4461, doi:10.1029/2002JD003183.

Miller, J. B., K. A. Mack, R. Dissly, J. W. C. White, E. J. Dlugokencky, and P. Tans (2002), Development of analytical methods and measurements of $^{13}C/^{12}C$ in atmospheric CH_4 from the NOAA Climate Monitoring and Diagnostics Laboratory Global Air Sampling Network, *J. Geophys. Res.*, *107*(D13), 4178, doi:10.1029/2001JD000630.

Platt, U., W. Allan, and D. Lowe (2004), Hemispheric average Cl atom concentration from the $^{13}C/^{12}C$ ratios in atmospheric methane, *Atmos. Chem. Phys.*, *4*, 2393–2399.

Quay, P. D., et al. (1991), Carbon isotopic composition of atmospheric CH_4: Fossil and biomass burning source strengths, *Global Biogeochem. Cycles*, *5*(1), 25–47.

Quay, P., J. Stutsman, D. Wilbur, A. Snover, E. Dlugokencky, and T. Brown (1999), The isotopic composition of atmospheric methane, *Global Biogeochem. Cycles*, *13*(2), 445–461.

Reeburgh, W. S. (2004), Global methane biogeochemistry, in *The Atmosphere*, edited by R. F. Keeling, pp. 65–90, Elsevier, New York.

Rice, A., A. A. Gotoh, H. O. Aijie, and S. Tyler (2001), High-precision continuous-flow measurements of $\delta^{13}C$ and δD of atmospheric CH_4, *Anal. Chem.*, *73*, 4104–4110.

Rice, A., S. Tyler, M. C. McCarthy, K. A. Boering, and E. Atlas (2003), Carbon and hydrogen isotopic compositions of stratospheric methane: 1. High-precision observation from the NASA ER-2 aircraft, *J. Geophys. Res.*, *108*(D15), 4460, doi:10.1029/2002JD003042.

Rommelaere, V., L. Arnaud, and J.-M. Barnola (1997), Reconstructing recent atmospheric trace gas concentrations from polar firn and bubble ice data by inverse methods, *J. Geophys. Res.*, *102*(D25), 30,069–30,083.

Santrock, J., S. A. Studley, and J. M. Hayes (1985), Isotopic analyses based on the mass spectrum of carbon dioxide, *Anal. Chem.*, *57*, 1444–1448.

Schwander, J., B. Stauffer, and A. Sigg (1988), Air mixing in firn and the age of the air at pore close-off, *Ann. Glaciol.*, *10*, 141–145.

Schwander, J., J.-M. Barnola, C. Andrie, M. Leuenberger, A. Ludin, D. Raynaud, and B. Stauffer (1993), The age of the air in the firn and the ice at Summit, Greenland, *J. Geophys. Res.*, *98*(D2), 2831–2838.

Sowers, T. A., and J. Jubenville (2000), A modified extraction technique for liberating occluded gases in ice cores, *J. Geophys. Res.*, *105*(D23), 29,155–29,164.

Sowers, T. A., M. L. Bender, and D. Raynaud (1989), Elemental and isotopic composition of occluded O_2 and N_2 in polar ice, *J. Geophys. Res.*, *94*(D4), 5137–5150.

Sowers, T., A. Rodebaugh, N. Yoshida, and S. Toyoda (2002), Extending records of the isotopic composition of atmospheric N_2O back to 1800 A.D. from air trapped in snow at South Pole and the Greenland Ice Sheet Project II ice core, *Global Biogeochem. Cycles*, *16*(4), 1129, doi:10.1029/2002GB001911.

Tans, P. (1997), A note on isotopic ratios and the global atmospheric methane budget, *Global Biogeochem. Cycles*, *11*(1), 77–81.

Taylor, K. C., et al. (2004), Abrupt climate change around 22 ka on the Siple Coast of Antarctica, *Quat. Sci. Rev.*, *23*, 7–15.

Trudinger, C. M., I. G. Enting, D. M. Etheridge, R. J. Francey, V. A. Levchenko, L. P. Steele, D. Raynaud, and L. Arnaud (1997), Modeling air movement and bubble trapping in firn, *J. Geophys. Res.*, *102*(D6), 6747–6764.

Tyler, S., H. O. Ajie, M. L. Grupta, R. J. Cicerone, D. R. Blake, and E. J. Dlugokencky (1999), Stable carbon isotopic composition of atmospheric methane: A comparison of surface level and free tropospheric air, *J. Geophys. Res.*, *104*(D11), 13,895–13,910.

Wang, J. S., M. B. McElroy, C. M. Spivakovsky, and D. B. A. Jones (2002), On the contribution of anthropogenic Cl to the increase in $\delta^{13}C$ of atmospheric methane, *Global Biogeochem. Cycles*, *16*(3), 1047, doi:10.1029/2001GB001572.

Whiticar, M. J. (1993), Stable isotopes and global budgets, in *Atmospheric Methane: Sources, Sinks, and Role in Global Change*, edited by M. A. K. Khalil, pp. 138–167, Springer, New York.

Whiticar, M. J. (2000), Can stable isotopes and global budgets be used to constrain atmospheric methane budgets, in *Atmospheric Methane*, edited by M. A. K. Khalil, pp. 63–85, Springer, New York.

Whiticar, M. J., E. Faber, and M. Schoell (1986), Biogenic methane formation in marine and freshwater environments: CO_2 reduction vs. acetate

fermentation—Isotope evidence, *Geochim. Cosmochim. Acta*, *50*, 693–709.

O. Aballain, J.-M. Barnola, S. Bernard, and J. Chappellaz, Laboratoire de Glaciologie et Géophysique de l'Environnement (CNRS-UJF), 54 rue Molière, Domaine Universitaire, BP 96, F-38042 St. Martin d'Hères, France. (oaballain@20minutes.fr; barnola@lgge.obs.ujf-grenoble.fr; bernard@lgge.obs.ujf-grenoble.fr; jerome@lgge.obs.ujf-grenoble.fr)

T. Marik, Institute of Environmental Physics, University of Heidelberg, Heidelberg, Germany. (thomas@marik.de)

T. Sowers, Department of Geosciences and the Earth and Environmental Systems Institute, Pennsylvania State University, 237 Deike Building, University Park, PA 16802, USA. (sowers@geosc.psu.edu)

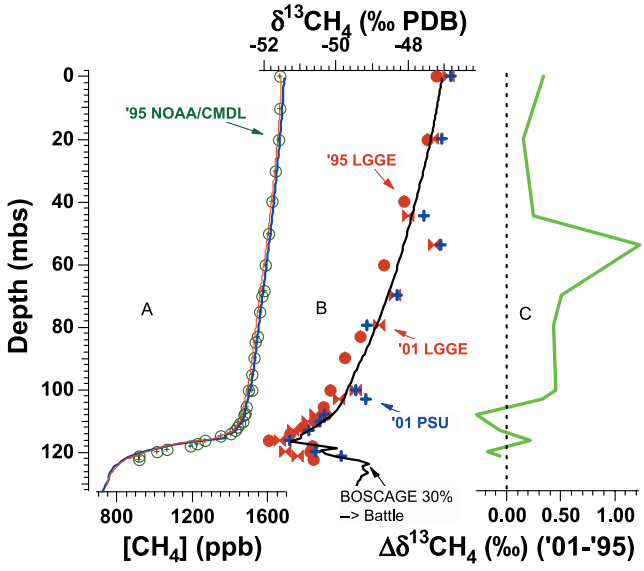

Figure 2. Results of CH_4 and $\delta^{13}CH_4$ analyses on South Pole Firn air. (a) CH_4 data were measured on the 1995 samples at NOAA/CMDL (P. Tans, personal communication, 2002). The red and blue lines are the model predicted CH_4 profiles from the *Battle et al.* [1996] (blue) and *Rommelaere et al.* [1997] (red) firn models. (b) The $\delta^{13}CH_4$ measurements at LGGE (red, 1995 and 2001) and PSU (blue, 2001 only). Also plotted with a solid black line is the inferred firn air $\delta^{13}CH_4$ profile (2001) using the BOSCAGE-8 atmospheric output with 30% of total biomass burning assigned to anthropogenic activities and the *Battle et al.* [1996] firn air model. (c) The $\Delta\delta^{13}CH_4$ data are the difference between the 2001 and 1995 LGGE data.

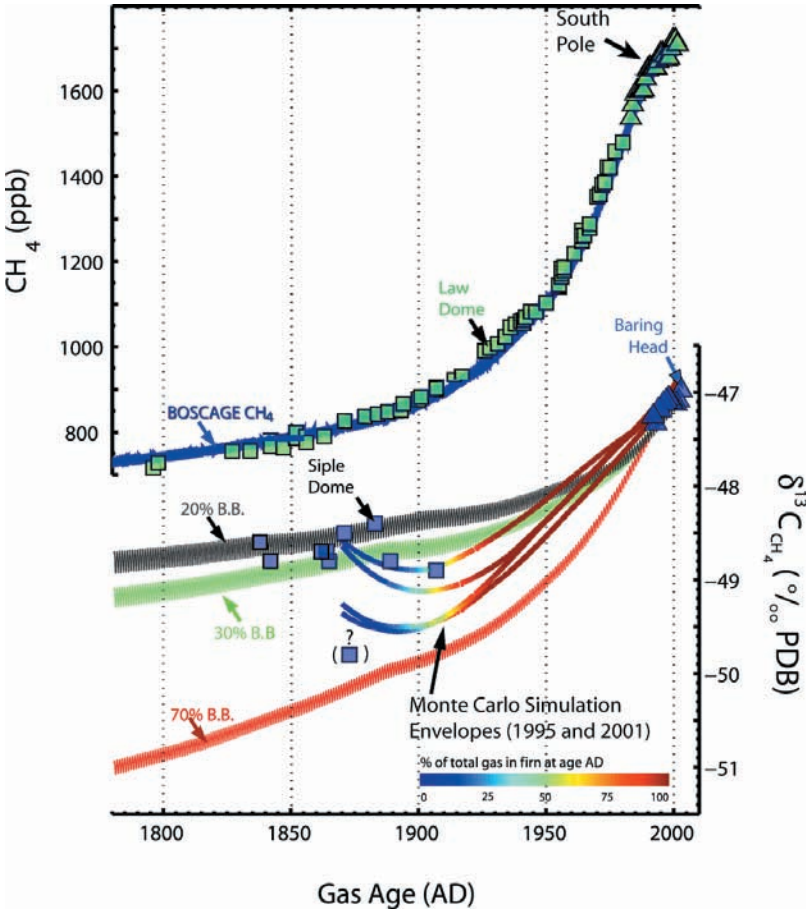

Figure 3. Records of $[CH_4]$ and $\delta^{13}CH_4$ covering the last 2 centuries: (top) $[CH_4]$ data from *Etheridge et al.* [1998] along with the resulting BOSCAGE predicted curve, and (bottom) model records of $\delta^{13}CH_4$ versus time, ice core data from Siple Dome, and direct atmospheric measurements from Baring Head [*Lowe et al.*, 1994]. Maximum and minimum curves of the Monte Carlo simulations are plotted with color lines. The color coding corresponds to the percent of air in the firn that is represented at the corresponding historical date. One Siple Dome $\delta^{13}CH_4$ value from 66.5 mbs (1873 A.D.) is considered questionable as it was 1‰ lower than the other nine samples. Also plotted are three BOSCAGE simulations with varying percentages of biomass burning CH_4 attributed to anthropogenic activities. The model simulations with 20–30% of biomass burning attributed to anthropogenic activities is in agreement with the Siple Dome and Monte Carlo simulation from South Pole firn air.